Developmental Biology 323 (2008) 166–176

Contents lists available at ScienceDirect

Developmental Biology

journal homepage: www.elsevier.com/developmentalbiology

Tissue-specific functions of the *Caenorhabditis elegans* p120 Ras GTPase activating protein GAP-3

Attila Stetak [1], Peter Gutierrez, Alex Hajnal *

Institute of Zoology, University of Zürich, Winterthurerstr. 190, CH-8057 Zürich, Switzerland

ARTICLE INFO

Article history:
Received for publication 22 May 2008
Revised 26 August 2008
Accepted 27 August 2008
Available online 5 September 2008

Keywords:
Ras
GTPase
GAP
Tumor
Suppressor

ABSTRACT

All metazoan genomes encode multiple RAS GTPase activating proteins (RasGAPs) that negatively regulate the conserved RAS/MAPK signaling pathway. In mammals, several RasGAPs exhibit tumor suppressor activity by preventing excess RAS signal transduction. We have identified *gap-3* as the to date missing *Caenorhabditis elegans* member of the p120 RasGAP family. By studying the genetic interaction of *gap-3* with the two previously identified RasGAPs *gap-1* and *gap-2*, we find that different combinations of RasGAPs are used to repress LET-60 RAS signaling depending on the cellular context. GAP-3 is the predominant negative regulator of RAS during meiotic progression of the germ cells, while GAP-1 is the key inhibitor of RAS during vulval induction. In other tissues such as the sex myoblasts or the chemosensory neurons, all three RasGAPs act in concert. The *C. elegans* RasGAPs have thus undergone partial specialization after gene duplication to allow the differential regulation of the RAS/MAPK signaling pathway in different cell types. A similar tissue specialization of the human tumor suppressor genes may explain the strong bias in the type of cancer they promote when mutated.

Introduction

Growth factor signals play a central role in controlling cellular proliferation, growth and differentiation. The production and release of specific growth factors by the signal sending cells must therefore be tightly controlled. However, it is equally important to turn off intracellular signal transduction in the signal receiving cells after growth factor stimulation to ensure an appropriate magnitude and duration of the response.

RAS proteins act as the central switch in many growth factor-stimulated signaling pathways. Aberrant RAS activation caused by activating point mutations in one of the three human *ras* genes or in the gene encoding their downstream target B-Raf occurs in a large proportion of human tumors (Dhillon et al., 2007; Rajalingam et al., 2007). RAS proteins bind and hydrolyze GTP into GDP, which allows RAS to function as binary switch oscillating between the active, GTP-bound and inactive, GDP-bound conformation. Ras GTPase activating proteins (RasGAPs) stimulate the weak intrinsic GTP hydrolyzing activity of RAS, thereby shifting the balance from the active, GTP-bound towards the inactive, GDP-bound state. The human genome encodes 11 different RasGAP proteins that form four sub-families based on their conserved domain composition (Bernards, 2003). The first RasGAP discovered was a widely expressed mammalian protein called p120 or RASA1 (Trahey and McCormick, 1987). Homologs of p120 RasGAP have been identified in most vertebrates as well as in *Drosophila melanogaster* (*Vap*), but not in yeast (Botella et al., 2003). p120 RasGAPs have a typical domain structure composed of a Src homology 3 (SH3) domain flanked by two SH2 domains, followed by a pleckstrin homology (PH), a C2 domain and a C-terminal catalytic domain found in all RasGAP families (Fig. 1B) (Bernards, 2003).

In addition to the p120 sub-family of RasGAPs, most eukaryotic genomes encode one or several members of each the Neurofibromin 1 (NF1), the synGAP and the Gap1 sub-families of RasGAPs. In particular, members of the Gap1 sub-family have previously been identified in *Caenorhabditis elegans* (*gap-1*) and *Drosophila* (*gap1*) as negative regulators of receptor tyrosine kinase (RTK)-activated RAS/MAPK signaling pathways that control vulval and eye development, respectively (Gaul et al., 1992; Hajnal et al., 1997). Besides the previously described Gap1 (*gap-1*) and synGAP (*gap-2*), no p120 RasGAP ortholog has so far been found in *C. elegans*, and there appears to be no clear NF1 ortholog either.

The RAS/MAPK signaling pathway acts in multiple tissues at different developmental stages of *C. elegans* development. LET-60 RAS signaling has been extensively studied during vulval cell fate specification where three out of six equipotent epithelial vulval precursor cells (VPCs, P3.p through P8.p) adopt two distinct vulval cell fates (Kornfeld, 1997; Sternberg and Horvitz, 1986). The anchor cell (AC) in the somatic gonad releases an inductive epidermal growth factor signal (LIN-3) and thereby induces the nearest VPC (P6.p) to generate eight descendants that form the center of the developing vulva, a lineage designated the primary (1°) cell fate (Kimble, 1981; Sternberg and Horvitz, 1986). The inductive AC signal activates in P6.p

* Corresponding author. Fax: +41 1 6356878.
E-mail address: ahajnal@zool.unizh.ch (A. Hajnal).
[1] Present address: Department of Developmental Biology, Utrecht University, Padualaan 8, 3584 CH Utrecht, The Netherlands.

0012-1606/$ – see front matter © 2008 Elsevier Inc. All rights reserved.
doi:10.1016/j.ydbio.2008.08.026

an evolutionary conserved receptor tyrosine RAS/MAP kinase signaling pathway (for review see Kornfeld, 1997). The neighboring VPCs (P5.p and P7.p) receive a lateral signal from P6.p that inactivates the RAS/MAPK pathway and instructs the 2° cell fate (Berset et al., 2001; Yoo et al., 2004). Most of the core components of the *C. elegans* RAS/MAPK pathway have been identified through genetic screens for mutations causing defects in vulval development. The LIN-3 EGF signal is received in P6.p by the LET-23 receptor tyrosine kinase, which is similar to the vertebrate EGF receptor (ErbB1) (Aroian et al., 1990). *sem-5* encodes an adaptor protein similar to vertebrate GRB2 (Clark et al., 1992) that binds to the activated LET-23 EGF receptor and recruits the guanine nucleotide exchange factor SOS-1 to the plasma membrane (Chang et al., 2000), where it can activate the single *C. elegans* RAS protein termed LET-60 (Beitel et al., 1990; Han et al., 1990). *lin-45*, *mek-2,* and *mpk-1* encode proteins similar to RAF, MEK, and MAP kinase, respectively, that transduce the inductive signal downstream of RAS (Han et al., 1993; Kornfeld et al., 1995; Lackner et al., 1994; Wu and Han, 1994; Wu et al., 1995).

In addition to vulval cell fate specification, LET-60 RAS signaling is required for the specification of the duct cell in the excretory system. *let-60* loss-of-function mutants lack an excretory duct cell and die as "rod-like" L1 larvae due to defective osmoregulation (Yochem et al., 1997). Moreover, LET-60 RAS signaling is needed in chemosensory neurons for the detection of volatile attractants (Hirotsu et al., 2000), in the germ cells for progression through the pachytene stage of meiosis I (Church et al., 1995), in the migrating sex myoblasts to control their final position around the vulva (Sundaram et al., 1996), for the specification of the P12 cell fate in the posterior ectoderm (Jiang and Sternberg, 1998) and for the formation of the tail spicule in males (Chamberlin and Sternberg, 1994). Different RTKs activate RAS signaling in different tissues. LET-23 EGFR acts upstream of LET-60 RAS in the VPCs, the excretory duct, the P12 cell and the male tail, the EGL-15 FGF receptor activates RAS during sex myoblast migration and the upstream activators of RAS in the germ cells and the chemosensory neurons are unknown.

Several genes encoding negative regulators of the RTK/RAS/MAPK pathway have been identified through mutations causing excess

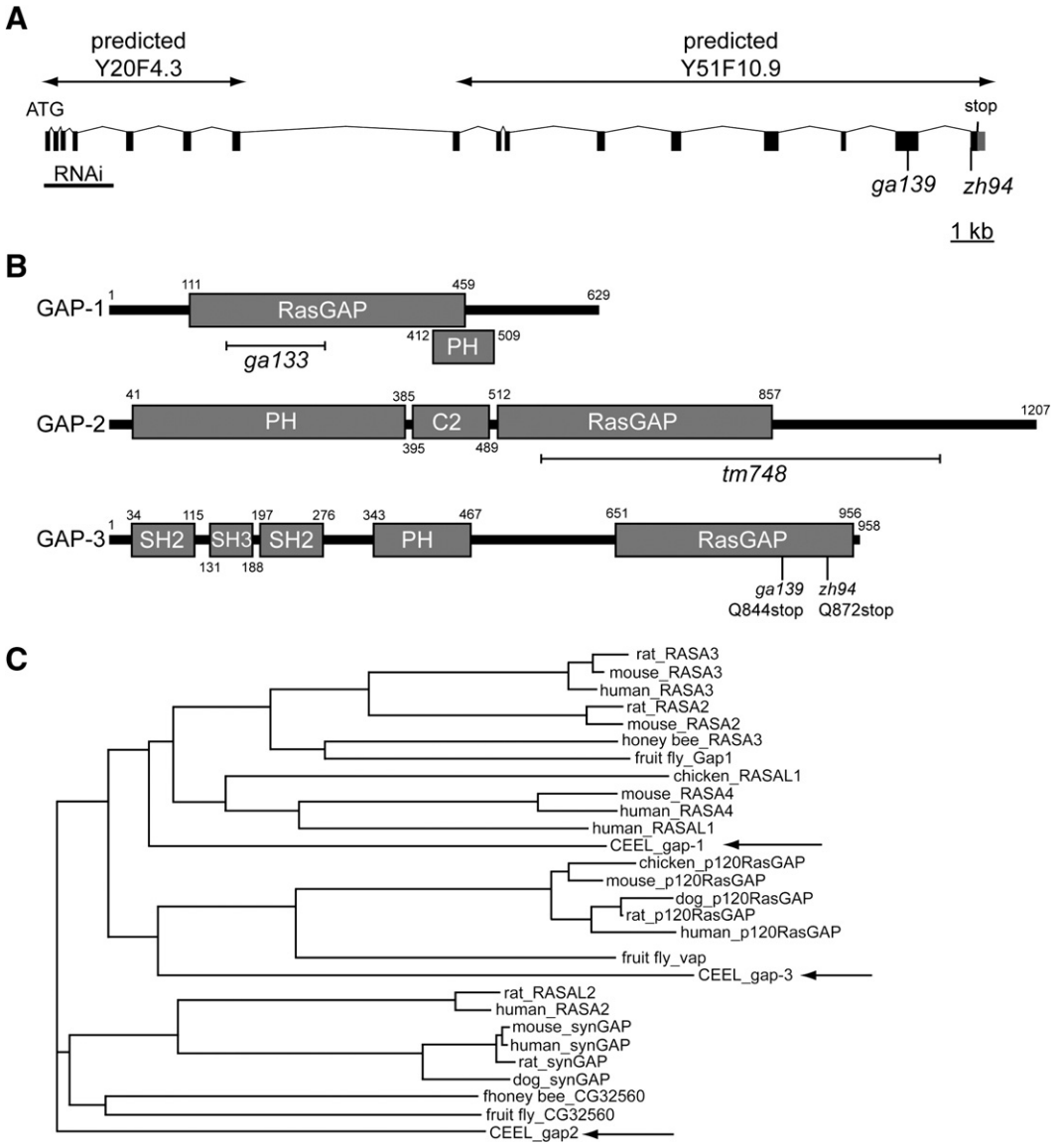

Fig. 1. (A) Genomic organization of the *gap-3* gene. The two predicted ORFs Y20F4.3 and Y51F10.9 encode the *gap-3* transcript as shown in Suppl. Fig. s1. The locations of the *ga139* and *zh94* amber mutations and the fragment used for RNAi are indicated. (B) Domain organization of the three *C. elegans* RasGAP proteins GAP-1, GAP-2 and GAP-3. The positions of the deletion alleles of GAP-1 and GAP-2 and the stop mutations in GAP-3 used for this study are shown. (C) Phylogenic analysis of selected RasGAPs from the Gap1, the p120 and the synGAP sub-families in mammals, insects and *C. elegans*. A phylogenic tree was constructed from the full-length protein sequences using the program ClustalW, where clades for subclasses were supported with >90% bootstrap values. The arrows point at the three *C. elegans* RasGAPs.

Table 1
RasGAPs during vulval induction

Row	Genotype	% Muv[a]	% Vul[b]	I[c]	% of VPCs induced[d]						*n*	*U*-test[e]
					P3.p	P4.p	P5.p	P6.p	P7.p	P8.p		
1	*gap-1(ga133)*	0	0	3.0	0	0	100	100	100	0	Many	–
2	*gap-2(tm748)*	0	0	3.0	0	0	100	100	100	0	48	–
3	*gap-3(ga139)*	0	0	3.0	0	0	100	100	100	0	35	–
4	*gap-1(ga133) gap-2(tm748)*	0	0	3.0	0	0	100	100	100	0	52	–
5	*gap-3(ga139); gap-1(ga133)*	71	0	4.03	20	65.7	100	100	100	17	35	$4.2*10^{-11}$ (1)
6	*gap-3(zh94); gap-1(ga133)*	64	0	3.79	9.7	45.2	100	100	100	24.2	31	$2.0*10^{-6}$ (1)
7	*gap-3(ga139); gap-2(tm748)*	0	0	3.0	0	0	100	100	100	0	26	–
8	*gap-1(ga133); gap-3 RNAi*	13.6	0	3.14	0	6.8	100	100	100	6.8	44	0.08 (1)
9	*let-60(n1876)*	0	100	0	0	0	0	0	0	0	27	–
10	*let-60(n1876); gap-1(ga133)*	5.4	0	3.05	0	2.7	100	100	100	2.7	37	$1.1*10^{-11}$ (9)
11	*let-60(n1876); gap-2(tm748)*	0	100	0.01	0	0	0	4	0	0	26	0.81 (9)
12	*gap-3(ga139); let-60(n1876)*	0	100	0.08	0	0	0	8.1	0	0	37	0.59 (9)
13	*let-60(n2021)*	0	17	2.66	0	0	88.3	92.6	85.1	0	47	–
14	*let-60(n2021); gap-1(ga133)*	0	0	3.0	0	0	100	100	100	0	44	0.083 (13)
15	*let-60(n2021); gap-2(tm748)*	0	18.75	2.75	0	0	85.4	99	91	8.3	48	0.97 (13)
16	*gap-3(ga139); let-60(n2021)*	0	0	3.0	0	0	100	100	100	0	39	0.087 (13)
17	*sem-5(n2019)*	0	75	1.1	0	0	35.9	39.1	34.4	0	64	–
18	*gap-1(ga133) sem-5(n2019)*	0	0	3.0	0	0	100	100	100	0	30	$5.2*10^{-9}$ (17)
19	*sem-5(n2019) gap-2(tm748)*	0	69.8	1.28	0	0	40.7	47.7	39.5	0	43	0.48 (17)
20	*gap-3(ga139); sem-5(n2019)*	0	44.2	2.02	0	0	65	75.6	61.6	0	43	$4.8*10^{-4}$ (17)

Numbers in brackets indicate the row to which a dataset was compared. *n* indicates the number of animals scored.
[a] %Muv indicates the fraction of animals with more than three induced VPCs.
[b] %Vul indicates the fraction of animals with fewer than three induced VPCs.
[c] The induction index I indicates the average number of VPCs per animal that adopted 1° or 2° fates as described (Berset et al., 2001).
[d] % of VPCs induced indicates for each VPC the fraction of cells adopting a 1° or 2° fate.
[e] Statistical significance was tested with Mann–Whitney *U*-test.

vulval induction. These inhibitors act either at the level of the LET-23 EGFR, such as the Cbl ortholog SLI-1 (Yoon et al., 1995), the Ack-related receptor tyrosine kinase ARK-1 (Hopper et al., 2000) or the receptor tyrosine phosphatase DEP-1 (Berset et al., 2005), on the LET-60 RAS protein, such as GAP-1 (Hajnal et al., 1997), and at the level of the MAP kinase MPK-1, such as the dual-specificity phosphatase LIP-1 (Berset et al., 2001) or the LST-1 protein (Yoo et al., 2004). Single mutations in any of those negative regulators do not cause obvious phenotypes. Only when two or more inhibitors are lost, a similar phenotype as in RAS gain-of-function mutants can be observed.

We have thus used *gap-1* null mutants to isolate new inhibitors of the RAS/MAPK pathway and identified a mutation in the *C. elegans* p120-type RasGAP *gap-3* that has previously not been found due to an incomplete annotation of the *C. elegans* genome. By systematically analyzing the tissue-specific interactions between the three *C. elegans* RasGAPs, we find that depending on the cellular context different combinations of RasGAPs are used to down-regulate RAS signaling. Our results indicate that during metazoan evolution the RasGAPs have undergone partial specialization after gene duplication.

Materials and methods

General methods and strains used

Standard methods were used for maintaining and manipulating *C. elegans* (Brenner, 1974); all experiments were conducted at 20 °C. The *C. elegans* Bristol strain, variety N2, was used as the wild-type reference strain in all experiments. The mutations used have been described previously (Brenner, 1974) and are listed by their linkage group.

LG I: *gap-3(ga139)*, *gap-3(zh94)* (this study); LG II: *rrf-3(pk1426)* (Simmer et al., 2002); LG III: *unc-119(e2498)* (Maduro and Pilgrim, 1995); LG IV: *let-60(n2021)*, *let-60(n1876)* (Beitel et al., 1990), *let-60 (ga89)* (Eisenmann and Kim, 1997); LG X: *gap-1(ga133)* (Hajnal et al., 1997), *gap-2(tm748)* (Hayashizaki et al., 1998), *sem-5(n2019)* (Clark et al., 1992). Extrachromosomal transgenic array: *zhEx161[pAS-96; punc-119+]*.

The pAS-96 (*gap-3p::NLS::LacZ::GFP*) transcriptional reporter was generated by PCR amplification of a genomic fragment containing 5 kb of 5′ promoter sequence and the first 4 exons of the open reading frame using the primers (GTTAGTGTATACGCACAGACG and CTCTCAACTGATTTCG-CATG) and cloned into the PstI and MscI sites of pPD95.67 expression vector (kind gift of A. Fire).

Transgenic lines were generated by injecting the plasmid pAS-96 at a concentration of 100 ng/μl into both arms of the syncytial gonad as described (Mello et al., 1991). *punc-119* was used as a transformation marker at 20 ng/μl concentration.

RNAi experiments were done by feeding worms with double-stranded RNA producing bacteria as described (Kamath et al., 2001).

Northern-blot analysis

Five micrograms of mixed stage worm total RNA was separated by formaldehyde denaturing agarose gel electrophoresis and transferred to hybond N+ nylon membrane (Amersham, Piscataway, New Jersey, USA). The membrane was probed with a radiolabeled 500 bp N-terminal cDNA fragment of *Y20F4.3* gene under stringent conditions.

Phenotypic analyses of gap mutants

Vulval induction was scored by examining worms at the L4 stage under Nomarski optics as described (Berset et al., 2001). The number of VPCs that had adopted a 1° or 2° vulval fate was counted for each animal, and the induction index was calculated by dividing the number of 1° or 2° induced cells by the number of animals scored.

Excretory duct cell specification was scored by direct observation under Nomarski optics in L4 larvae. The number of the duct cell(s) was determined according to position and morphology as shown in Fig. 4.

Sex myoblast (SM) migration was scored using Nomarski optics microscopy as described previously (Sundaram et al., 1996). Individual SM positions were assessed relative to a compartment defined by the closest VPC. If SM and/or VPC had divided the midway of the two daughter cells was used as reference point.

P12 differentiation was scored in L3 hermaphrodites using Nomarski optics microscopy. P11 and P12 fates were determined according to the distinct nuclear morphologies and positions of P11.p and P12.pa cells as described (Hajnal et al., 1997).

L1 viability was quantified by transferring a defined number of eggs (between 48 and 52) to an unseeded NGM plate. 24 h later, hatched viable and "rod-like" dead L1 larvae were counted using a dissecting microscope.

To score pachytene exit, one day old adult animals were methanol fixed for 5 min in siliconized Eppendorf tubes, air dried and re-hydrated with PBS containing Hoechst dye (1:1000 dilution of the saturated stock). Following the removal of the staining solution, samples were mounted on glass slides in Mowiol. Quantification was performed using the Openlab 5.0 software by measuring the distance from the posterior end of the gonad bend to the first diakinesis nucleus as determined by the characteristic morphology of the bivalent chromosomes visualized with DAPI staining. Data were statistically analyzed by two-tailed Student's *t*-test.

Chemotaxis assays were conducted on 10 cm CTX plates with well-fed synchronized young adult worms as described (Nuttley et al., 2002). The worms were given a choice between a spot of diacetyl diluted to a concentration of 0.01% or 0.1% (vol/vol) in ethanol with 20 mM sodium azide and a counter spot with ethanol and sodium azide. Before the assays, the animals were washed twice in water by letting them settle by gravity, and 100–200 worms were placed in the center of the CTX plates in 50 µl ddH_20. After 1 h the animals were counted and a chemotaxis index was calculated as described (Bargmann et al., 1993).

Results

gap-3 encodes a RasGAP of the p120 family

To identify novel negative regulators of the EGFR/RAS/MAPK signaling pathway in *C. elegans*, we have previously performed a genetic screen for mutations that cause excess vulval induction and a multivulva (Muv) phenotype in a sensitized *gap-1(ga133)* loss-of-function background (Canevascini et al., 2005). *gap-1* encodes a RAS GTPase-activating protein (RasGAP) that inhibits LET-60 RAS signaling, but *gap-1(ga133)* single mutants develop a wild-type vulva (Figs. 3A, J and Table 1, row 1) (Hajnal et al., 1997). The *ga139* mutation recovered in this screen causes a penetrant Muv and slightly dumpy (Dpy) phenotype in the *gap-1(ga133)* background, but no obvious vulval phenotype as a single mutant (Table 1, row 3, 5 and Figs. 3C, D, L). The mutation was mapped to the left arm of chromosome I to an 86 kilobase (kb) interval containing 15 candidate genes (Suppl. Fig. s1A). RNA interference against the predicted open reading frame *Y20F4.3* phenocopied the *ga139* synthetic Muv phenotype (Fig. 1A, Table 1, row 8). Since the *Y20F4.3* transcript was only predicted by the Genefinder program, but not confirmed by expressed sequence tags (ESTs), we performed Northern-blot analysis from total wild-type (N2) RNA to determine the actual size of the transcript (Suppl. Fig. s1B). Using a 500 base pair (bp) N-terminal probe for *Y20F4.3*, we detected a single band that migrated at a molecular mass of approximately 4 kb which was larger than the predicted 1.2 kb mRNA. Using an SL1-specific primer to amplify the 5′ end in an RT-PCR reaction, we determined the sequence of the actual mRNA and found that the predicted ORFs *Y20F4.3* and *Y51F10.9* are in fact spliced together using a splice site within the last exon of the *Y20F4.3* gene thus excluding the predicted stop codon at the end of this exon. This produces a single transcript encoding an mRNA of 3029 bp with an ORF of 958 amino acids distributed over 16 exons (Fig. 1A, Suppl. Figs. s1A, C, Suppl. Fig. s2A,). Sequencing of the *Y20F4.3/Y51F10.9* gene in *ga139* animals revealed a G to A transition in exon 15 that changes a Glu residue into an amber stop codon and truncates the protein at amino acid 844 (Figs. 1A, B). In an independent screen, we isolated the *zh94* allele that causes a similar synthetic Muv phenotype with *gap-1(ga133)* as *ga139*, maps to the same region on LGI and fails to complement *ga139* (Table 1, row 6 and data not shown). Sequencing of the *gap-3* locus in *zh94* animals identified a C to T transition at the beginning of exon 16 replacing a Glu residue at position 872 with a stop codon (Figs. 1A, B).

The protein encoded by the combined *Y20F4.3* and *Y51F10.9* ORFs is a member of the RasGAP family carrying one SH3, two SH2, a pleckstrin homology (PH) and a RasGAP domain (Fig. 1B). It is most

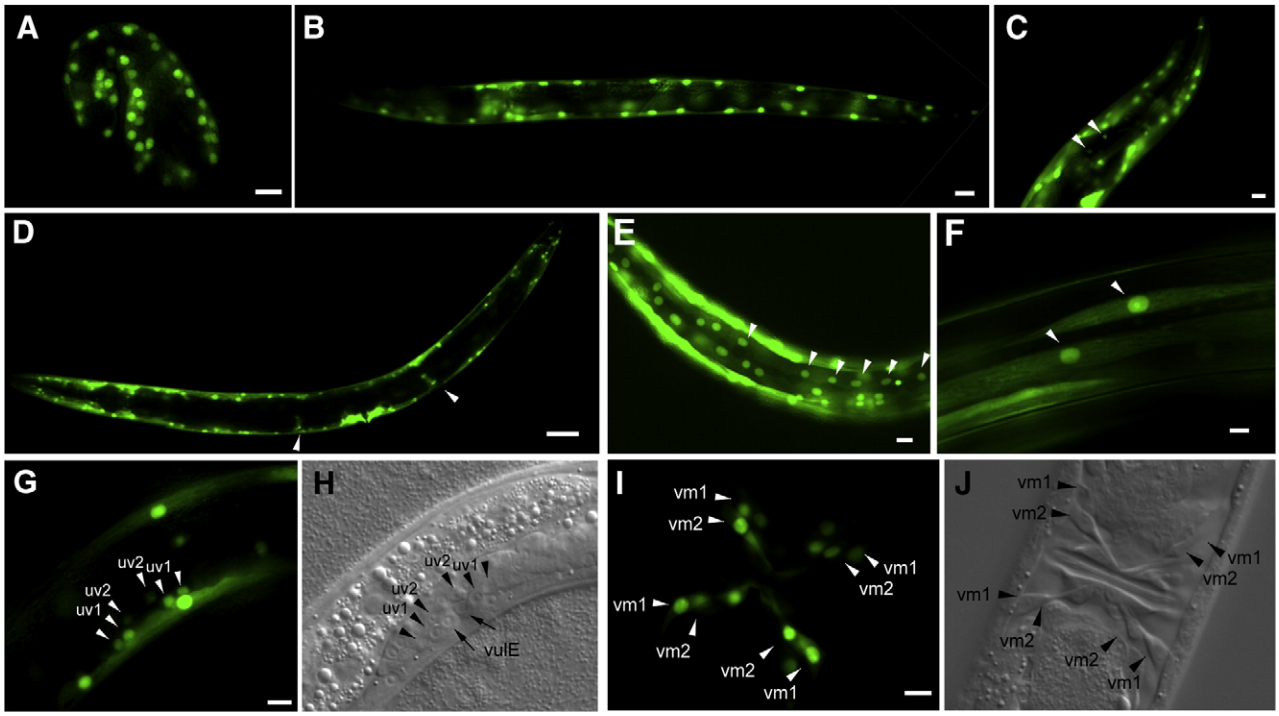

Fig. 2. Expression pattern of a transcriptional *gap-3::gfp* reporter. (A) *gap-3::gfp* expression in 1.5-fold stage embryos, (B) expression in an L1 larva, which persists throughout larval development until (D) adulthood. *gap-3::gfp* was detected (C) in some neurons of the nerve ring (arrowheads) (D), the spermatheca (arrowheads) (scale bar is 50 µm), (E) the seam cells (arrowheads), (F) the body wall muscles (arrowheads), (G, H) the uv1 and uv2 vulva-uterine cells (arrowheads), and (I, J) the vm1 and vm2 sex muscles (arrowheads). Scale bars in panels A–C and E–H are 10 µm.

similar to members of the p120 RasGAP family, while the two other RasGAPs previously identified in *C. elegans*, GAP-1 and GAP-2, belong to RasGAP-like and synRasGAP sub-families, respectively (Fig. 1C, Suppl. Fig. s2B) (Bernards, 2003). We thus named the gene mutated in *ga139* and *zh94* animals *gap-3*. Since the *gap-3(ga139)* mutation removes part of the RasGAP domain (amino acids 844 to 956), it likely destroys the catalytic activity of GAP-3 and may represent a null allele with respect to the RasGAP activity. Using forward genetics, we have thus identified *gap-3* as the single *C. elegans* member of p120 RasGAP family.

A. transcriptional gap-3 reporter is widely expressed during different stages of development

We next analyzed the expression pattern of *gap-3* by fusing 5 kilobase (kb) of 5′ upstream sequence to a *nls::gfp::lacZ* reporter cassette. This transcriptional *gap-3* reporter was expressed throughout *C. elegans* development and first detected in ball stage embryos. At the 1.5-fold stage, the GFP signal was observed mainly in hypodermal cells (Fig. 2A), and expression persisted throughout larval development until adulthood (Figs. 2B, D). Furthermore, the *gap-3* reporter was expressed in some head neurons (Fig. 2C), in the spermatheca (Fig. 2D), in the seam cells (Fig. 2E), in the body wall muscles (Fig. 2F), and in the sex muscles of the adult hermaphrodite (Figs. 2I, J). We also observed expression in some uterine cells (Figs. 3G, H) but did not detect a GFP signal in the vulval cells, the excretory duct cell or the P12.p cell at any developmental stage. Similar to *gap-3*, transcriptional reporters for *gap-1* and *gap-2* are widely expressed in many tissues at different stages (Hayashizaki et al., 1998 and data not shown).

GAP-1 is the predominant negative regulator of LET-60 RAS during vulval induction

The identification of *gap-3* as the *C. elegans* p120 RasGAP and the availability of null alleles for *gap-1* and *gap-2* opened the possibility to test the tissue-specificity and functional redundancy between members of the three major classes of RasGAPs in an animal model. We first examined the function of the three *gap* genes during vulval fate specification. As single mutants, each of the three *gaps* exhibits a wild-type vulval phenotype (Figs. 3A–C, J, K and Table 1, rows 1–3). To investigate the functional redundancy between the three RasGAPs, we generated all *gap* double mutant combinations and analyzed the vulval induction at the L4 larval stage (Figs. 3D–F and Table 1, rows 4–7). We could not generate homozygous *gap* triple mutants, most likely

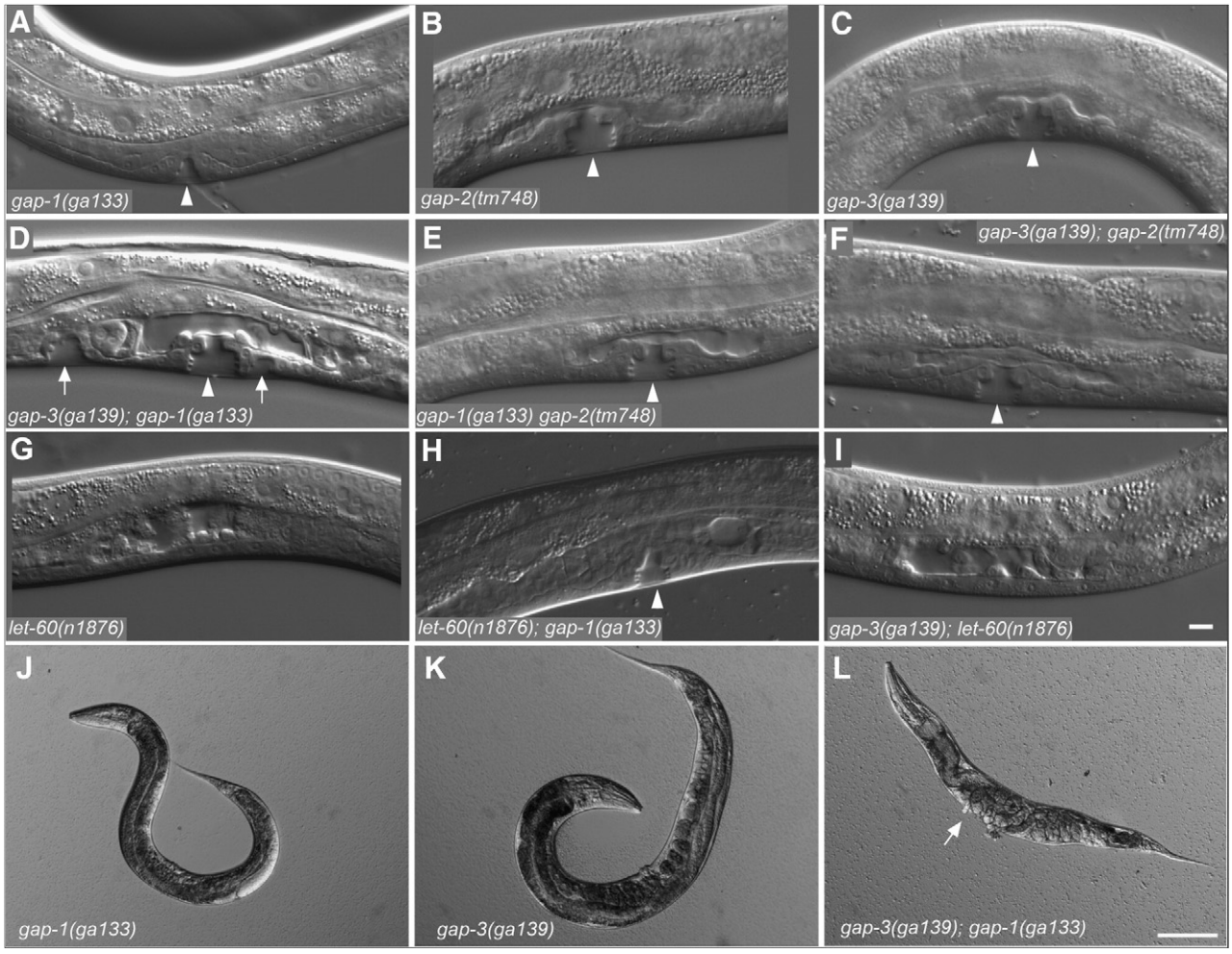

Fig. 3. GAP-1 and GAP-3 act redundantly during vulval development. Lateral views of the mid-body region of mid-L4 stage hermaphrodites showing the developing vulva (indicated by arrowheads) in (A) *gap-1(ga133)*, (B) *gap-2(tm748)*, (C) *gap-3(ga139)* single mutants, which all developed a wild-type vulva formed by the descendants of P5.p, P6.p and P7.p. (D) A *gap-3(ga139); gap-1(ga133)* double mutant containing two pseudovulvae indicated by arrows flanking the normal vulva. (E) *gap-1(ga133); gap-2(tm748)* and (F) *gap-3(ga139); gap-2 (tm748)* double mutants always contain one normal vulva. (G) The *let-60(n1876)* Vul phenotype is suppressed by (H) *gap-1(ga133)* (arrowhead) but neither by (I) *gap-3(ga139)* nor by *gap-2(tm748)* (not shown). (J) Lower magnification images of a *gap-1(ga133)*, (K) a *gap-3(ga139)* single and (L) a *gap-3(ga139); gap-1(ga133)* double mutant. The arrow in panel L indicates the position of a pseudovulva. Scale bars in panels I and L are 10 μm and 100 μm, respectively.

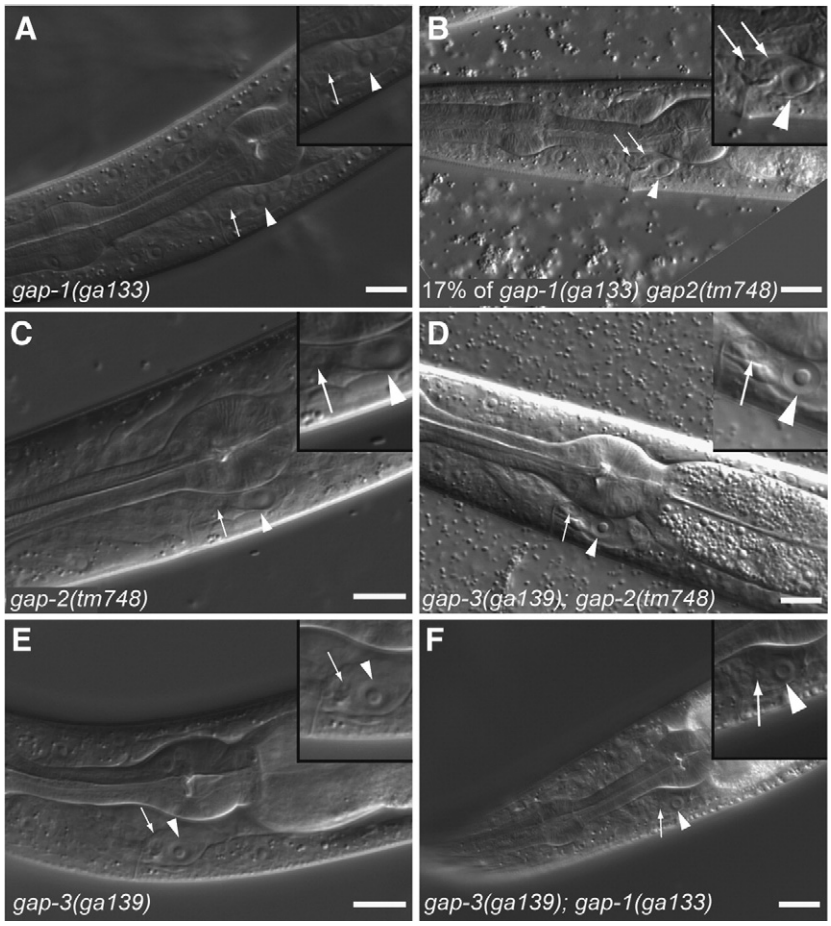

Fig. 4. GAP-1 and GAP-2 are the predominant inhibitors of LET-60 RAS during excretory duct cell specification. In all panels, lateral views of the head region in adult hermaphrodites show the excretory cells (arrowheads) and excretory duct cells (arrows) with higher magnifications in the insets. (A) *gap-1(ga133)* single mutant with one and (B) *gap-1(ga133); gap-2(tm748)* double mutant with two duct cells (arrows, 17% of the cases, $n=64$). (C) *gap-2(tm748)* single, (D) *gap-3(ga139); gap-2(tm748)* double, (E) *gap-3(ga139)* single and *gap-3(ga139); gap-1(ga133)* double mutants all contain a single duct cell. Scale bar is 10 μm.

because loss of all three *gaps* causes an early lethal phenotype (data not shown). Only *gap-1(ga133); gap-3(ga139)* double mutants exhibited a Muv phenotype, suggesting that these two RasGAPs are functionally redundant during vulval induction (Figs. 3D, L and Table 1, rows 5, 6). Furthermore, *gap-1(ga133)* completely suppressed the Vul phenotype of two *let-60* alleles (*n2021* and *n1876*) (Fig. 3H and Table 1, rows 9, 10, 13, 14) as well as of the reduction-of-function mutation in *sem-5*, which encodes a GRB2-like adaptor protein (Table 1, rows 17, 18). In contrast, *gap-3(ga139)* only partially suppressed the *sem-5(n2019)* Vul phenotype (Table 1, rows 17, 20) and had no effect on the stronger *let-60(n1876)* allele (Fig. 3I and Table 1, rows 9, 12). *gap-2(tm748)* was unable to suppress any of the three Vul mutants tested (Table 1, rows 11, 15, 19), confirming the previous report indicating that GAP-2 has no function during vulval cell fate specification (Hayashizaki et al., 1998). Thus, GAP-1 is the main negative regulator of LET-60 RAS signaling during vulval induction, while GAP-3 plays a comparably minor and GAP-2 no detectable role during vulval development.

Excretory duct cell specification is mainly controlled by GAP-1 and GAP-2

During development, LET-60 RAS signaling controls the specification of the excretory duct cell that is required for proper osmoregulation by connecting the excretory cell to the excretory pore cell. *let-60 ras* loss-of-function mutants lack the excretory duct cell and die as "rod-like" larvae probably due to an excretion defect (Yochem et al., 1997). Hyperactivation of LET-60 RAS often causes the formation of two excretory duct cells, but *gap* single mutants always had a single duct cell (Figs. 4A, C, E) (Berset et al., 2005). In 17.2% of the cases ($n=64$), *gap-1(ga133)*; *gap-2(tm748)* double mutants contained two excretory duct cells (Fig. 4B), while none of the other two double mutant combinations showed a duct cell duplication phenotype (Figs. 4D, F). We further tested the role of the RasGAPs in the excretory duct cell specification by analyzing the L1 viability of *let-60(rf)*; *gap* double mutant animals. All three RasGAPs partially suppressed the lethality of the strong *let-60(n1876)* allele, but *gap-1(ga133)* was the most potent suppressor (Table 2, rows 2–4). Surprisingly, *gap-1(ga133)* was not able to suppress the weaker

Table 2
RasGAPs during excretory duct cell specification

Row	Genotype	% Viable L1[a]	*n*	χ^{2b}
1	*let-60(n1876)*	28%	71	–
2	*let-60(n1876); gap-1(ga133)*	76.7%	60	$1.8*10^{-15}$ (1)
3	*let-60(n1876); gap-2(tm748)*	52%	25	$1.3*10^{-6}$ (1)
4	*gap-3(ga139); let-60(n1876)*	51.9%	27	$1.4*10^{-6}$ (1)
5	*let-60(n2021)*	65.3%	144	–
6	*let-60(n2021); gap-1(ga133)*	67.7%	196	0.52 (5)
7	*let-60(n2021); gap-2(tm748)*	93.7%	142	$1.7*10^{-12}$ (5)
8	*gap-3(ga139); let-60(n2021)*	90.2%	133	$4.1*10^{-9}$ (5)

Numbers in brackets indicate the row to which a dataset was compared. *n* indicates the number of animals scored.
[a] % Viable L1 indicates the fraction of living L2 animal.
[b] Statistical significance was tested with χ^2 test.

let-60(n2021) allele, while *gap-2* and *gap-3* both efficiently suppressed the lethality associated with *let-60(n2021)* (Table 2, rows 6–8). The missense G75S mutation in *let-60(n2021)* is located in a highly conserved region of unknown function. Furthermore, this region is dispensable for oncogenic transformation of NIH3T3 cells by mutationally activated Ras (v-H-Ras) (Sigal et al., 1986). Therefore, one possible explanation for this allele-specific interaction is that GAP-1 activity in the excretory duct cell depends on an unknown tissue-specific co-factor that interacts with LET-60 RAS and that this interaction is perturbed by the missense G75S mutation in *let-60 (n2021)* but not by the T66A mutation in *let-60(n1876)* animals.

Taken together, we conclude that GAP-1 and GAP-2 are the major RasGAPs regulating the excretory duct cell specification, while GAP-3 plays a less prominent role in this process.

Redundant function of the three RasGAPs during sex myoblast migration

We noticed that *gap-1(ga133); gap-3(ga139)* double mutants exhibited a clear body (Clr) phenotype similar to mutations that hyperactivate the EGL-15 FGFR signaling pathway (Fig. 3L) (Kokel et al., 1998). This observation suggested that *gap-1* and *gap-3* may negatively regulate RAS signaling in the EGL-15 FGFR pathway. In particular, an FGF signal emanating from the VPCs activates via the fibroblast growth factor receptor EGL-15 and the GRB2 adapter SEM-5 a LET-60 RAS signaling pathway in the precursors of the sex muscles, the sex myoblasts (SMs) to control their proper positioning. The SMs are generated in the posterior half of the mid-body region and migrate to the anterior during the L2 larval stage to assume their final positions flanking the center of the developing gonad near the site of the future vulva (Sulston and Horvitz, 1977).

To quantify the role of *gap* genes in SM migration, we scored the positions of the SMs relative to the VPCs during the mid-L3 larval stage as described (Sundaram et al., 1996). The *gap* single or double mutants did not show any defects in SM migration (data not shown). We therefore tested the *gap* alleles for suppression of the SM migration defects caused by reduction-of-function mutations in the RAS pathway. Since the viable *let-60(rf)* alleles only cause mild defects in SM migration, we used the *sem-5(n2019)* mutation to reduce LET-60 RAS signaling in the SMs. While in 100% of wild-type animals the SMs terminated migration near P6.p, the SMs of *sem-5 (n2019)* mutants were positioned only in 56.7% of the cases nearest to P6.p, and they displayed a much broader pattern of anterior–posterior distribution (Table 3, row 1, 2). Analysis of *sem-5(n2019); gap* double mutants indicated that the *gap-1(ga133), gap-2(tm748)* and *gap-3(ga139)* mutations all suppressed the *sem-5(n2019)* SM positioning defect to a similar extent (Table 3 rows 3, 4, 5). Therefore, the three RasGAPs make an equal contribution to controlling LET-60 RAS signaling during SM migration.

Table 3
RasGAP proteins during sex myoblast migration

Row	Genotype	P3.p	P4.p	P5.p	P6.p	P7.p	P8.p	*n*	χ^{2a}
1	*Wild-type*	–	–	–	100%	–	–	Many	–
2	*sem-5(n2019)*	–	–	3.3%	56.7%	33.3%	6.7%	30	$3.1*10^{-7}$ (1)
3	*gap-1(ga133) sem-5(n2019)*	–	–	–	83.3%	16.7%	–	24	$1.6*10^{-5}$ (2)
4	*sem-5(n2019) gap-2(tm748)*	–	–	–	89.5%	10.5%	–	19	$1.4*10^{-12}$ (2)
5	*gap-3(ga139); sem-5(n2019)*	–	–	10%	80%	10%	–	30	$1.9*10^{-13}$ (2)

Relative position of the sex myoblast compared to the VPCs in L3 animals as described previously (Sundaram et al., 1996).
Numbers in brackets indicate the row to which a dataset was compared. *n* indicates the number of animals scored.
[a] Statistical significance was tested with χ^2 test.

Table 4
RasGAPs during P12 specification

Row	Genotype	P12→P11[a]	*n*	χ^{2b}
1	*let-60(n1876)*	10.6%	47	–
2	*let-60(n1876); gap-1(ga133)*	0%	40	$4.0*10^{-117}$ (1)
3	*let-60(n1876); gap-2(tm748)*	6.9%	29	0.55 (1)
4	*gap-3(ga139); let-60(n1876)*	2.8%	36	$5.5*10^{-5}$ (1)
5	*sem-5(n2019)*	36.8%	38	–
6	*gap-1(ga133) sem-5(n2019)*	10.2%	49	$1.2*10^{-16}$ (5)
7	*sem-5(n2019) gap-2(tm748)*	31%	29	0.66 (5)
8	*gap-3(ga139); sem-5(n2019)*	25%	44	0.059 (5)

Numbers in brackets indicate the row to which a dataset was compared. *n* indicates the number of animals scored.
[a] Percentage of animals where P12 to P11 cell transformation occurred. P11 and P12 fates were determined according to the distinct nuclear morphologies and positions of P11.p and P12.pa cells.
[b] Statistical significance was tested with χ^2 test.

Specification of the P12 cell fate is mainly controlled by GAP-1

The P12 cell is the most posterior cell of the ventral cord precursors (Sulston and Horvitz, 1977). A LIN-3 EGF signal transduced by the EGFR/RAS/MAPK pathway is required for P12 to execute a specific neuro-ectoblast fate. In the absence of the LIN-3 EGF signal, P12 instead adopts the fate of its neighbor P11 (Jiang and Sternberg, 1998). Similar to the SM migration, *gap* single or double mutants did not show a P12 cell fate transformation (data not shown). We thus analyzed the ability of the *gap* mutations to suppress the P12 specification defects observed in the *let-60(n1876)* and the *sem-5 (n2019)* backgrounds. Since homozygous *let-60(n1876)* animals segregate 100% dead L1 larvae due to the lack of the excretory duct cell, only the maternally rescued F1 progeny of a heterozygous *let-60 (n1876)* parent could be scored. These maternally rescued *let-60 (n1876)* animals exhibited a partial defect in P12 cell fate specification that was completely suppressed by the *gap-1(ga133)* mutation but not by *gap-2(tm748)* and only partially by *gap-3(ga139)* (Table 4, rows 1–4). Similarly, the P12 specification defect of *sem-5(n2019)* animals was significantly suppressed by the *gap-1(ga133)* mutation, but not by *gap-2(tm748)* and only marginally by *gap-3(ga139)* (Table 4, rows 5–8). We thus conclude that similar to vulval induction, GAP-1 is the predominant RasGAP used during P12 cell differentiation.

GAP-3 is the predominant negative regulator of LET-60 RAS signaling in the germline

Activation of a RAS/MAPK signaling pathway in the distal syncytial gonad arm promotes the transition of germ cells through the pachytene stage of the first meiotic prophase. Germ cells normally exit pachytene when they arrive at the flexure of the gonad and are in diakinesis when they enter the proximal gonad arm. At this stage, the chromosomes are further condensed, the germ cell nuclei become cellularized, and their cytoplasmic volume increases rapidly as they develop into oocytes (Figs. 5A, I) (Hirsh et al. 1976).

Hyperactivation of the RAS/MAPK pathway through a *let-60* gain-of-function mutation or a loss-of-function mutation in the MAPK phosphatase *lip-1* causes premature pachytene exit, resulting in an increased number of smaller cellularized germ cells that accumulate in multiple layers in the proximal gonad arm (Fig. 5B). Interestingly, already *gap-3(ga139)* single mutants showed a weak premature pachytene exit phenotype similar to *let-60(ga89gf)* animals (Figs. 5B, G) (Eisenmann and Kim, 1997). In fact, this is the only single mutant phenotype we observed in any of the *gap(lf)* mutants. This premature pachytene exit phenotype was further enhanced in *gap-3(ga139); gap-1(ga133)* double mutant animals (Fig. 5H). On the other hand, *gap-1 (ga133) gap-2(tm748)* double mutants exhibited no obvious defect in the germline, and *gap-2(tm748)* did not enhance the *gap-3(ga139)* phenotype (Figs. 5C–F).

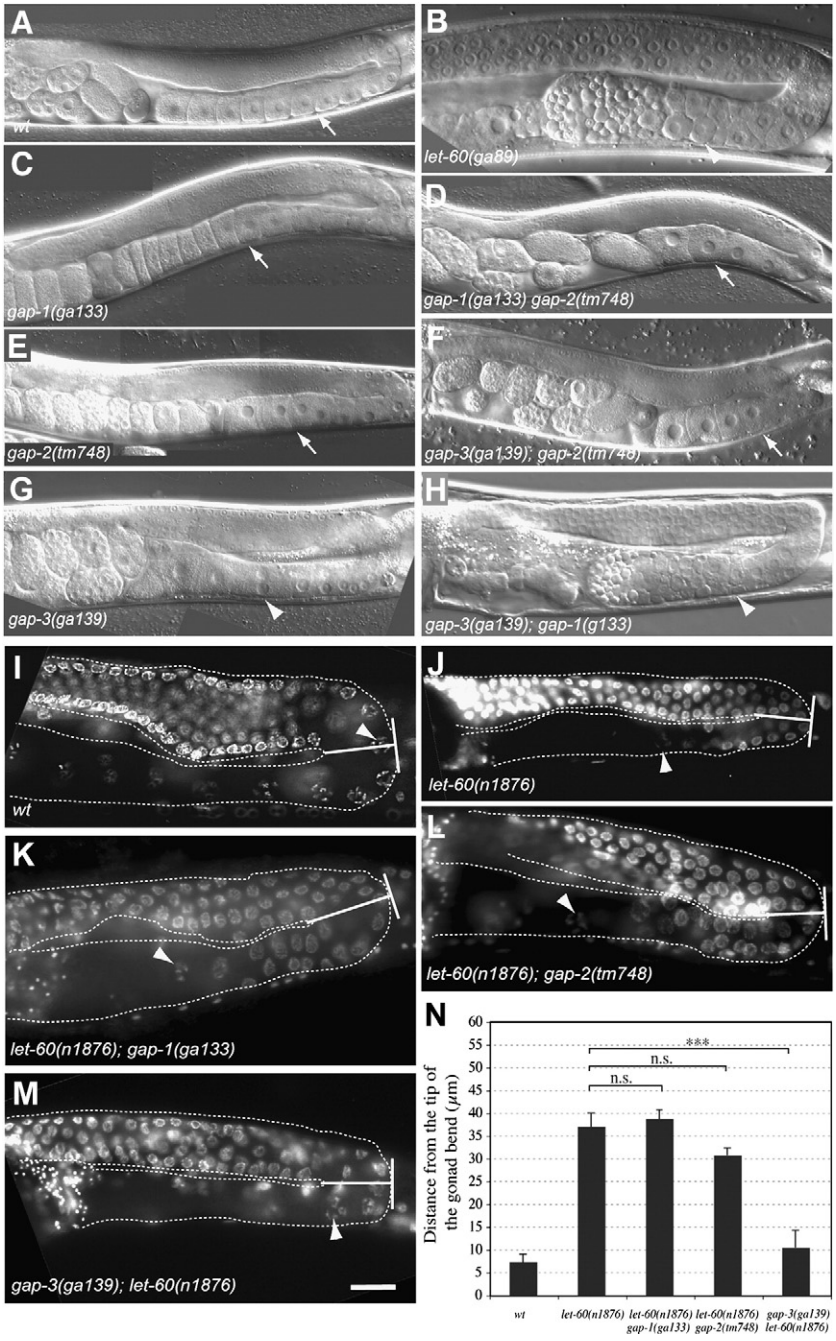

Fig. 5. GAP-3 is the main regulator of LET-60 RAS in pachytene stage germ cells. Lateral views of the posterior gonad arms in adult hermaphrodites are shown. (A) Note the single row of oocytes in the proximal gonad arm of wild-type animals (arrow). (B) In the *let-60(ga89)* gain-of-function mutant increased number of smaller oocytes in the proximal gonad arm accumulates in multiple rows on top of each other (arrowhead). (C) In *gap-1(ga133)* single, (D) *gap-1(ga133); gap-2(tm748)* double, (E) *gap-2(tm748)* single and (F) *gap-3(ga139); gap-2(tm748)* double mutants the proximal gonad arms show no obvious defect (arrows). (G) In *gap-3(ga139)* single mutants some oocytes are stacked in multiple rows indicating a mild defect (arrowhead). (H) *gap-3(ga139); gap-1(ga133)* double mutants exhibit strong pachytene exit defects similar to the *let-60(ga89gf)* mutants shown in panel B (arrowhead). (I) DAPI stained adult gonads to determine the site of pachytene exit in wild-type, (J) *let-60(n1876rf)* single and (K) *let-60(n1876rf); gap-1(ga133)*, (L) *let-60(n1876rf); gap-2(tm748)* and (M) *gap-3(ga139); let-60(n1876rf)* double mutants. The first diakinesis nuclei (arrowheads) normally appear in the region where the gonad turns anterior. Scale bar is 10 μm. (N) Quantification of the pachytene exit defects. The distance between first diakinesis nucleus (arrowheads in panels I–M) and the turn of the gonad arm (white bars in panels I–M) was measured. Statistical significance was tested by two-tailed Student's *t*-test where *** indicates $p<0.001$. Error bars indicate the s.d. of 10 to 27 animals for each genotype.

In the strong *let-60(n1876)* reduction-of-function mutant, the reduced RAS activity delays pachytene exit and causes the accumulation of pachytene stage nuclei in the proximal gonad arm (Fig. 5J) (Church et al., 1995). On average, in *let-60(n1876)* animals pachytene stage germ cell nuclei were found in the proximal gonad arm up to 37±4 μm past the gonadal turn ($n=12$) (Figs. 5J, N). This phenotype was suppressed in *gap-3(ga139); let-60(n1876)* double mutant animals (Figs. 5M, N) ($n=12$), while *gap-1(ga133)* ($n=10$) and *gap-2 (tm748)* ($n=27$) both had no effect on the pachytene exit defect of *let-60(n1876)* animals (Figs. 5K, L, N). In summary, our data indicate that LET-60 RAS signaling during germ cell development is largely controlled by the p120 RasGAP GAP-3 with only a small contribution by GAP-1.

All three RasGAPs regulate chemotaxis to volatile attractants

C. elegans possesses three bilateral pairs of chemosensory neurons to detect a wide variety of volatile substances. LET-60 RAS activity in

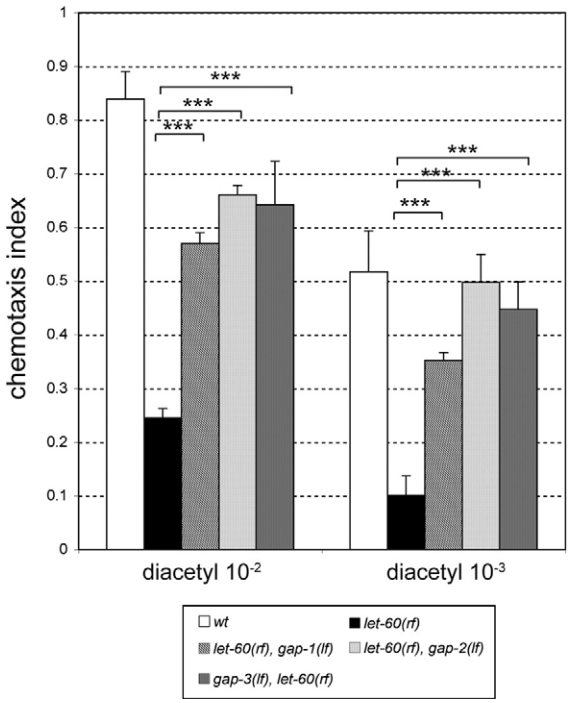

Fig. 6. All three RasGAPs inhibit LET-60 RAS during chemosensation. Chemotaxis towards two concentrations of diacetyl as attractant was tested for suppression of the *let-60(n2021rf)* chemotaxis defect. Statistical significance was tested by a two-tailed Student's *t*-test where *** indicates $p<0.001$. Error bars indicate the s.d. observed in three independent experiments done in triplicate.

the chemosensory neurons is required for sensing volatile attractants. Reduced LET-60 signaling impairs chemotaxis towards volatile attractants such as isoamylalcohol or diacetyl (Hirotsu et al., 2000). We therefore tested the ability of each of the three *gap(lf)* mutations to suppress the *let-60(n2021)* chemotaxis defect using diacetyl as attractant. In all three *let-60(n2021); gap(lf)* double mutants, chemotaxis towards diacetyl was nearly restored to wild-type levels (Fig. 6). Thus, the three RasGAPs together regulate LET-60 RAS signaling during chemosensation.

Discussion

A tight regulation of the RAS/MAPK signaling pathways is necessary to control many different aspects of animal development and adult life. RasGAPs are key negative regulators that can act constitutively or in negative feedback loops to prevent excess RAS signal transduction, and they possess tumor suppressor activity in mice and humans (Bernards and Settleman, 2005). The genomes of all metazoans encode multiple RasGAPs that have arisen through several rounds of gene expansion and loss during evolution and can be grouped into four sub-families (Jiang and Ramachandran, 2006). Using forward genetics, we have identified *gap-3* as the *C. elegans* member of the p120 family of RasGAPs. The GAP-3 protein exhibits the domain composition and arrangement typical of p120 family RasGAPs, and it seems to be the only protein with these features encoded by the *C. elegans* genome. *C. elegans* thus contains single members for three of the four sub-families of RasGAPs that all inhibit the single RAS protein LET-60. For the fourth class, the Neurofibromin NF1-type RasGAPs, there appears to be no direct ortholog since the *C. elegans* synGAP GAP-2 shows the strongest similarity to human NF1. The availability of mutations in each of the three *C. elegans* RasGAPs has allowed us to investigate the tissue-specificity and redundancy of different RasGAP family members in an animal model.

So far, functional studies in animal models have implicated RasGAPs in a variety of specific processes during development and in adult behavior. Loss of murine p120 RasGAP, for example, results in embryonic lethality, abnormal vascularization and enhanced neuronal apoptosis (Henkemeyer et al., 1995). Similarly, mutants in the *Drosophila* p120 GAP ortholog *vap* show age-related brain degeneration (Botella et al., 2003). Homozygous *NF1* deficient mice display embryonic lethality due to heart malformation (Jacks et al., 1994), while *Drosophila NF1* mutants show an overall growth deficiency, defects in long-term memory formation (Walker et al., 2006), a loss of the escape response (The et al., 1997) and lack a circadian rest-activity rhythm (Williams et al., 2001). The different RasGAP family members thus exhibit a high degree of functional specialization and tissue-specificity, suggesting that different RasGAPs are used to control RAS signaling depending on the cellular context.

In contrast to *Drosophila* and vertebrates, single mutations in the three *C. elegans* RasGAPs do not show obvious phenotypes, whereas gain-of-function mutations in the *let-60 ras* gene cause readily detectable defects in various tissues. The only exception is the mild pachytene exit defect observed in the germline of *gap-3(lf)* single mutants. On the other hand, the different *gap* double mutant combinations we tested uncovered inhibitory activities for at least one of the three RasGAPs in most if not all of the tissues where *let-60 ras* has been reported to function (Fig. 7). The three *C. elegans* RasGAPs therefore display a higher degree of redundancy than the RasGAPs in other animals. However, their individual contribution to the negative regulation of LET-60 RAS signaling in the different tissues is not equal, as specific combinations of GAPs are used depending on the cellular context (Fig. 7). All three RasGAPs contribute almost equally to control

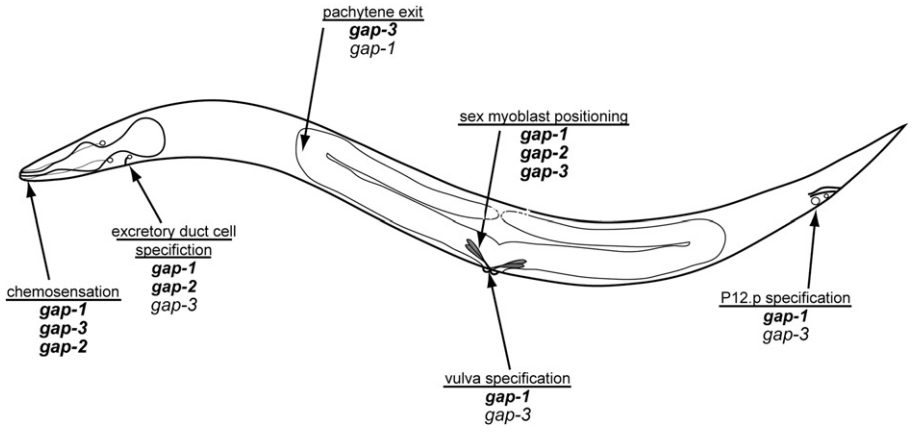

Fig. 7. Tissue-specificity of the three *C. elegans* RasGAPs. For each of the tissues analyzed, the RasGAP(s) with the strongest contribution are shown in bold letters.

RAS signaling during sex myoblast positioning and chemosensation, but only GAP-1 and GAP-3 are used to repress LET-60 RAS during vulval development, while GAP-1 and GAP-2 are the main regulators of RAS during excretory duct cell specification. Even more striking are the cases of pachytene exit in the germline and P12 specification in the posterior ectoderm where GAP-3 and GAP-1, respectively, are the predominant RasGAPs (Fig. 7). Interestingly, the expression pattern of the individual RasGAPs does not reflect their tissue-specific functions. The absent expression of GAP-1 and GAP-3 in the vulval cells could be explained by a lack of specific regulatory elements in the reporter constructs used. However, strong expression of GAP-2 has been observed in the vulval cells and in the germline (Hayashizaki et al., 1998), yet GAP-2 does not have a detectable function in these two tissues. An alternative explanation for the tissue-specific functions could be that each RasGAP requires a specific co-factor expressed only in certain cell types in order to repress LET-60 RAS signaling. The observation that *gap-1(ga133)* efficiently suppresses the weak *let-60 (n2021)* allele in all tissues except for the excretory duct cell, although gap-1 does suppress the stronger *let-60(n1876)* allele in the duct cell, could be explained by a duct cell-specific co-factor for GAP-1 that fails to interact with the mutant LET-60(G75S) protein in *let-60(n2021)* animals.

A clear gradation and specification of the RasGAP family has occurred from yeast to vertebrates. The yeast genome encodes two members of the NF1 family IRA1 and IRA2 that act on RAS1 and are likely the product of a yeast-specific genome duplication (Parrini et al., 1996). A relatively simple metazoan such as the sea anemone *Nematostella vectensis*, a Cnidarian whose genome has recently been sequenced, already contains at least four different RasGAP genes, two members of the NF1 and the Gap1 sub-families each (A.S. and A.H., personal observation). The *Drosophila* genome encodes four RasGAP genes that represent one member of each sub-family, and vertebrate genomes typically encode multiple members of each RasGAP sub-family, indicating a further expansion of the RasGAPs at the base of the vertebrate tree. Those gene expansions in the RasGAP family may have allowed individual RasGAPs to take on more specialized functions in different cell types. The RasGAPs of *C. elegans* appear to be special in two important aspects. First, there are no discernible members of the NF1 sub-family in *C. elegans* or the closely related nematode *C. briggsae*, while the genome of the nematode *Pristionchus pacificus* encodes a clear NF1 ortholog (A.S. and A.H., personal observation). Thus, the NF1 class of RasGAPs has likely been lost in *C. elegans* and other closely related nematode species. Second, the higher degree of functional redundancy between the three RasGAPs in *C. elegans* compared to *Drosophila* or vertebrates suggests that the functional specification of the RasGAPs did not fully occur or may have been lost in *C. elegans*.

Many human tumor suppressor gene mutations exhibit a strong organ-specific bias in the type of cancer they induce when mutated. For example, mutations in the human p120 RasGAP RASA1 gene specifically cause capillary and arteriovenous malformation (Boon et al., 2005). This organ-specificity of tumor suppressor genes may be the consequence of a similar functional specification that has occurred during evolution of the conserved metazoan signaling pathways.

Acknowledgments

We wish to thank the members of our group for critical discussion and Lukas Neukomm and Claudia Walser for comments on the manuscript. We are grateful to Stuart Kim for providing us the *ga139* allele, Andrew Fire for GFP vectors, the *C. elegans* Genetics Centre and S. Mitani for providing strains. This research was supported by grants from Oncosuisse and the Swiss National Science foundation to A.H. and the Kanton of Zürich.

Appendix A. Supplementary data

Supplementary data associated with this article can be found, in the online version, at doi:10.1016/j.ydbio.2008.08.026.

References

Aroian, R.V., Koga, M., Mendel, J.E., Ohshima, Y., Sternberg, P.W., 1990. The *let-23* gene necessary for *Caenorhabditis elegans* vulval induction encodes a tyrosine kinase of the EGF receptor subfamily. Nature 348, 693–699.

Bargmann, C.I., Hartwieg, E., Horvitz, H.R., 1993. Odorant-selective genes and neurons mediate olfaction in *C. elegans*. Cell 74, 515–527.

Beitel, G.J., Clark, S.G., Horvitz, H.R., 1990. *Caenorhabditis elegans* ras gene *let-60* acts as a switch in the pathway of vulval induction. Nature 348, 503–509.

Bernards, A., 2003. GAPs galore! A survey of putative Ras superfamily GTPase activating proteins in man and *Drosophila*. Biochim. Biophys. Acta 1603, 47–82.

Bernards, A., Settleman, J., 2005. GAPs in growth factor signalling. Growth Factors 23, 143–149.

Berset, T., Hoier, E.F., Battu, G., Canevascini, S., Hajnal, A., 2001. Notch inhibition of RAS signaling through MAP kinase phosphatase LIP-1 during *C. elegans* vulval development. Science 291, 1055–1058.

Berset, T.A., Hoier, E.F., Hajnal, A., 2005. The *C. elegans* homolog of the mammalian tumor suppressor *Dep-1/Scc1* inhibits EGFR signaling to regulate binary cell fate decisions. Genes Dev. 19, 1328–1340.

Boon, L.M., Mulliken, J.B., Vikkula, M., 2005. RASA1: variable phenotype with capillary and arteriovenous malformations. Curr. Opin. Genet. Dev. 15, 265–269.

Botella, J.A., Kretzschmar, D., Kiermayer, C., Feldmann, P., Hughes, D.A., Schneuwly, S., 2003. Deregulation of the Egfr/Ras signaling pathway induces age-related brain degeneration in the *Drosophila* mutant vap. Mol. Biol. Cell 14, 241–250.

Brenner, S., 1974. The genetics of *Caenorhabditis elegans*. Genetics 77, 71–94.

Canevascini, S., Marti, M., Frohli, E., Hajnal, A., 2005. The *Caenorhabditis elegans*-oncogene *ect-2* positively regulates RAS signalling during vulval development. EMBO Rep. 6, 1169–1175.

Chamberlin, H.M., Sternberg, P.W., 1994. The *lin-3/let-23* pathway mediates inductive signalling during male spicule development in *Caenorhabditis elegans*. Development 120, 2713–2721.

Chang, C., Hopper, N.A., Sternberg, P.W., 2000. *Caenorhabditis elegans*-1 is necessary for multiple RAS-mediated developmental signals. Embo J. 19, 3283–3294.

Church, D.L., Guan, K.L., Lambie, E.J., 1995. Three genes of the MAP kinase cascade, *mek-2, mpk-1/sur-1* and *let-60 ras*, are required for meiotic cell cycle progression in *Caenorhabditis elegans*. Development 121, 2525–2535.

Clark, S.G., Stern, M.J., Horvitz, H.R., 1992. *C. elegans*-signalling gene sem-5 encodes a protein with SH2 and SH3 domains. Nature 356, 340–344.

Dhillon, A.S., Hagan, S., Rath, O., Kolch, W., 2007. MAP kinase signalling pathways in cancer. Oncogene 26, 3279–3290.

Eisenmann, D.M., Kim, S.K., 1997. Mechanism of activation of the *Caenorhabditis elegans* ras homologue *let-60* -sensitive, gain-of-function mutation. Genetics 146, 553–565.

Gaul, U., Mardon, G., Rubin, G.M., 1992. A putative Ras GTPase activating protein acts as a negative regulator of signaling by the Sevenless receptor tyrosine kinase. Cell 68, 1007–1019.

Hajnal, A., Whitfield, C.W., Kim, S.K., 1997. Inhibition of *Caenorhabditis elegans* vulval induction by *GAP-1* and *let-23* receptor tyrosine kinase. Genes Dev. 11, 2715–2728.

Han, M., Aroian, R.V., Sternberg, P.W., 1990. The *let-60* locus controls the switch between vulval and nonvulval cell fates in *Caenorhabditis elegans*. Genetics 126, 899–913.

Han, M., Golden, A., Han, Y., Sternberg, P.W., 1993. *C. elegans lin-45 raf* gene participates in *let-60 ras*-stimulated vulval differentiation. Nature 363, 133–140.

Hayashizaki, S., Iino, Y., Yamamoto, M., 1998. Characterization of the *C. elegans GAP-2* - GTPase activating protein and its possible role in larval development. Genes Cells 3, 189–202.

Henkemeyer, M., Rossi, D.J., Holmyard, D.P., Puri, M.C., Mbamalu, G., Harpal, K., Shih, T.S., Jacks, T., Pawson, T., 1995. Vascular system defects and neuronal apoptosis in mice lacking ras GTPase-activating protein. Nature 377, 695–701.

Hirotsu, T., Saeki, S., Yamamoto, M., Iino, Y., 2000. The Ras–MAPK pathway is important for olfaction in *Caenorhabditis elegans*. Nature 404, 289–293.

Hopper, N.A., Lee, J., Sternberg, P.W., 2000. ARK-1 inhibits EGFR signaling in *C. elegans*. Mol. Cell 6, 65–75.

Jacks, T., Shih, T.S., Schmitt, E.M., Bronson, R.T., Bernards, A., Weinberg, R.A., 1994. Tumour predisposition in mice heterozygous for a targeted mutation in Nf1. Nat. Genet. 7, 353–361.

Jiang, L.I., Sternberg, P.W., 1998. Interactions of EGF, Wnt and HOM-C genes specify the P12 neuroectoblast fate in *C. elegans*. Development 125, 2337–2347.

Jiang, S.Y., Ramachandran, S., 2006. Comparative and evolutionary analysis of genes encoding small GTPases and their activating proteins in eukaryotic genomes. Physiol. Genomics 24, 235–251.

Kamath, R.S., Martinez-Campos, M., Zipperlen, P., Fraser, A.G., Ahringer, J., 2001. Effectiveness of specific RNA-mediated interference through ingested double-stranded RNA in *Caenorhabditis elegans*. Genome Biol. 2 RESEARCH0002.

Kimble, J., 1981. Alterations in cell lineage following laser ablation of cells in the somatic gonad of *Caenorhabditis elegans*. Dev Biol. 87, 286–300.

Kokel, M., Borland, C.Z., DeLong, L., Horvitz, H.R., Stern, M.J., 1998. *clr-1* encodes a receptor tyrosine phosphatase that negatively regulates an FGF receptor signaling pathway in *Caenorhabditis elegans*. Genes Dev. 12, 1425–1437.

Kornfeld, K., 1997. Vulval development in *Caenorhabditis elegans*. Trends Genet. 13, 55–61.

Kornfeld, K., Guan, K.L., Horvitz, H.R., 1995. The *Caenorhabditis elegans* gene *mek-2* is required for vulval induction and encodes a protein similar to the protein kinase MEK. Genes Dev. 9, 756–768.

Lackner, M.R., Kornfeld, K., Miller, L.M., Horvitz, H.R., Kim, S.K., 1994. A MAP kinase homolog, *mpk-1*-mediated induction of vulval cell fates in *Caenorhabditis elegans*. Genes Dev. 8, 160–173.

Maduro, M., Pilgrim, D., 1995. Identification and cloning of *unc-119*, a gene expressed in the *Caenorhabditis elegans* nervous system. Genetics 141, 977–988.

Mello, C.C., Kramer, J.M., Stinchcomb, D., Ambros, V., 1991. Efficient gene transfer in *C. elegans*: extrachromosomal maintenance and integration of transforming sequences. Embo J. 10, 3959–3970.

Nuttley, W.M., Atkinson-Leadbeater, K.P., Van Der Kooy, D., 2002. Serotonin mediates food-odor associative learning in the nematode *Caenorhabditis elegans*. Proc. Natl. Acad. Sci. U. S. A. 99, 12449–12454.

Parrini, M.C., Bernardi, A., Parmeggiani, A., 1996. Determinants of Ras proteins specifying the sensitivity to yeast Ira2p and human p120-GAP. Embo J. 15, 1107–1111.

Rajalingam, K., Schreck, R., Rapp, U.R., Albert, S., 2007. Ras oncogenes and their downstream targets. Biochim. Biophys. Acta 1773, 1177–1195.

Sigal, I.S., Gibbs, J.B., D'Alonzo, J.S., Scolnick, E.M., 1986. Identification of effector residues and a neutralizing epitope of Ha-ras-encoded p21. Proc. Natl. Acad. Sci. U. S. A. 83, 4725–4729.

Simmer, F., Tijsterman, M., Parrish, S., Koushika, S.P., Nonet, M.L., Fire, A., Ahringer, J., Plasterk, R.H., 2002. Loss of the putative RNA-directed RNA polymerase RRF-3 makes *C. elegans* hypersensitive to RNAi. Curr. Biol. 12, 1317–1319.

Sternberg, P.W., Horvitz, H.R., 1986. Pattern formation during vulval development in *C. elegans*. Cell 44, 761–772.

Sulston, J.E., Horvitz, H.R., 1977. Post-embryonic cell lineages of the nematode, *Caenorhabditis elegans*. Dev. Biol. 56, 110–156.

Sundaram, M., Yochem, J., Han, M., 1996. A Ras-mediated signal transduction pathway is involved in the control of sex myoblast migration in *Caenorhabditis elegans*. Development 122, 2823–2833.

The, I., Hannigan, G.E., Cowley, G.S., Reginald, S., Zhong, Y., Gusella, J.F., Hariharan, I.K., Bernards, A., 1997. Rescue of a *Drosophila* NF1 mutant phenotype by protein kinase A. Science 276, 791–794.

Trahey, M., McCormick, F., 1987. A cytoplasmic protein stimulates normal N-ras p21 GTPase, but does not affect oncogenic mutants. Science 238, 542–545.

Walker, J.A., Tchoudakova, A.V., McKenney, P.T., Brill, S., Wu, D., Cowley, G.S., Hariharan, I. K., Bernards, A., 2006. Reduced growth of *Drosophila*-cell-autonomous requirement for GTPase-activating protein activity in larval neurons. Genes Dev. 20, 3311–3323.

Williams, J.A., Su, H.S., Bernards, A., Field, J., Sehgal, A., 2001. A circadian output in *Drosophila*-1 and Ras/MAPK. Science 293, 2251–2256.

Wu, Y., Han, M., 1994. Suppression of activated Let-60 ras protein defines a role of *Caenorhabditis elegans*-1 MAP kinase in vulval differentiation. Genes Dev. 8, 147–159.

Wu, Y., Han, M., Guan, K.L., 1995. MEK-2, a *Caenorhabditis elegans*-mediated vulval induction and other developmental events. Genes Dev. 9, 742–755.

Yochem, J., Sundaram, M., Han, M., 1997. Ras is required for a limited number of cell fates and not for general proliferation in *Caenorhabditis elegans*. Mol. Cell. Biol. 17, 2716–2722.

Yoo, A.S., Bais, C., Greenwald, I., 2004. Crosstalk between the EGFR and LIN-12/Notch pathways in *C. elegans* vulval development. Science 303, 663–666.

Yoon, C.H., Lee, J., Jongeward, G.D., Sternberg, P.W., 1995. Similarity of *sli-1*, a regulator of vulval development in *C. elegans*-oncogene c-cbl. Science 269, 1102–1105.